Exosome microarray based on label-free imaging biosensor

Yifei Wang¹, Wang Yuan², Qinming Zhang¹, Yixuan Wang¹, Michael Kimber², Liang Dong¹, and Meng Lu²

Department of Electrical and Computer Engineering,

Department of Biomedical Sciences,

Department of Mechanical Engineering,

Iowa State University, Ames, Iowa 50011, USA michaelk@iastate.edu, ldong@iastate.edu, menglu@iastate.edu

Abstract— Exosome vesicles (EVs) released by macrophages are potential biomarkers for the analysis of immune responses. This study reports a high-throughput EV detection assay developed using a label-free EV microarray. The EV microarray consists of a panel of seven antibodies that are specific to multiple membrane receptors of the target EVs. The EV microarray was fabricated on a photonic crystal (PC) biosensor surface. The hyperspectral imaging approached was implemented to quantify the antibody and EV absorptions on the PC-based microarray. The label-free EV microarray enables low-cost, rapid, and high-throughput characterization of macrophage EVs with a significantly reduced sample volume of 1 µL.

Keywords—Exosome Vesicles; microarray; hyperspectral imaging; label-free biosensor; photonic crystal

I. INTRODUCTION

Recent studies showed that exosomes vesicles (EVs) can transport a variety of molecular constituents, such as proteins, mRNA, and microRNAs, from their originating cells [1]. The analysis of circulating EVs in body fluids has emerged as a promising non-invasive molecular diagnostic method [2, 3]. The EVs secreted by macrophages are particularly interesting since the macrophage-derived EVs may play a role in immune system responses [4, 5]. The size of the macrophage-derived EVs ranges from 50 nm to 150 nm in diameter. These EVs can be isolated using centrifugation. To analyze the transmembrane receptors carried by these EVs, this study demonstrates the label-free EV microarray assay. The label-free EV microarray is built upon the photonic crystal (PC) sensor platform in conjunction with the hyperspectral imaging approach [6-10]. The EV microarray assay is designed to simultaneously measure seven membrane proteins of the macrophage-derived EVs using their corresponding antibodies printed on the EV microarray.

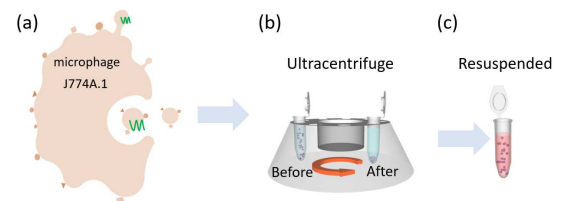


Fig. 1 Schematic flowchart of the EV isolation process. (a) Secretion of EVs from a macrophage cell. The EVs samples are (b) centrifuged and (c) resuspended before being pipetted onto the EV microarray.

II. MATERIAL AND METHODS

A. Preparation of EVs

Fig. 1 summarizes the major steps to collect EVs secreted by the macrophages (Fig. 1(a)) from cell line J774A.1 (TIB-67, ATCC). The J774A.1 cells were cultured for 24 hours before the medium was collected. Fig. 1(b) and (c) show the process of EV isolation from the culture medium by centrifugation and resuspension. The concentrations of the isolated EV samples were measured using a nanoparticle analysis tool (NanoSight LM10, Malvern Instruments).

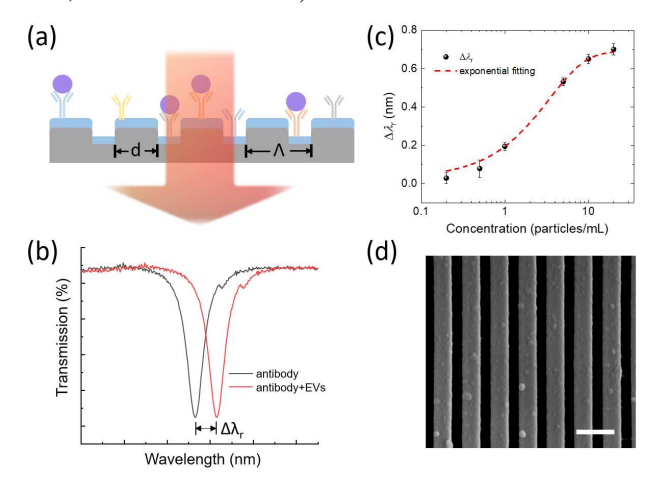


Fig. 2 Label-free detection of EVs using the PC biosensor. (a) Schematic diagram of the PC biosensor that is functionalized with the antibodies to recognize the target EVs. (b) Measured transmission spectra before and after the coating of the antibody. The spectral position of the minimal transmission represents the resonance wavelength. (c) Shifts of the resonance wavelength as a function of six different EV concentrations. The measured shift values are fitted to generate the dose-response curve. (d) SEM image of the EVs immobilized on the PC substrate. Scale bar: 500 nm.

B. Label-free microarray on PC biosensor

The PC biosensor used in this study consists of a onedimensional grating substrate coated with a 100-nm-thick thin film of titanium oxide (TiO₂) as shown in fig. 2(a). The highrefractive-index TiO₂ film acts as a light confinement layer to

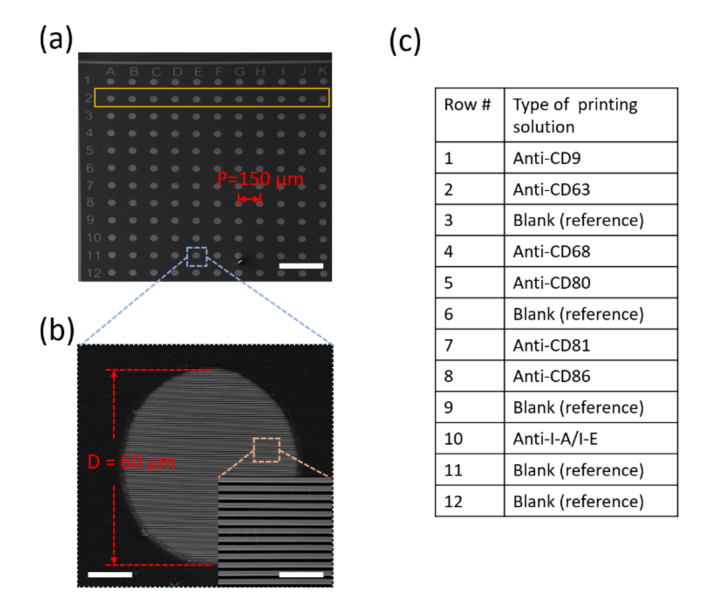


Fig. 3 Fabricated EV microarray. (a) SEM image of the array of 60-µm-diameter microwells patterned on the PC substrate using photolithography. Scale bar: 300 µm (b) SEM image of a single microwell with the grating pattern at the bottom. Scale bar: 15 µm (c) List of the printed antibodies and references with the corresponding row numbers.

support resonance modes, which have been exploited for the detection of biomaterials [11-13]. Illuminated by a board band excitation, the PC substrate exhibits narrow band optical resonances manifested by the dips in the transmission spectra as shown in fig. 2(b). On the PC surface, the absorption of the analyte, such as antibodies or EVs, can cause a wavelength shift, $\Delta \lambda$. of the resonance mode. The wavelength shift is proportional to the analyte concentration. Fig. 2(c) shows the measured dose-response curve of the macrophage-derived EVs. The EV concentrations ranged from $2 \times 10^{\circ}$ particles mL¹ to $2 \times 10^{\circ}$ particles mL², and the PC sensor was functionalized using

the CD-63 antibody. Fig. 2(d) shows the scanning electron microscope (SEM) image of the EVs on the PC substrate. The average size of EV is approximately 100 nm.

The EV microarray is designed to measure multiple membrane proteins carried by the EVs with a high throughput. The EV microarray was fabricated in two steps. Firstly, the microarray was patterned in a 1.5-µm-thick layer of photoresist (AZ 5214) on the PC substrate by photolithography. Fig. 3(a) shows the EV microarray with 11×12 microwells. The diameter and period of the microwell array is 60 μ m and 150 μ m, respectively. One microwell of the microarray is zoomed and shown in fig. 3(b). The inset SEM image elaborates the PC grating at the bottom of the microwell. Secondly, A molecular printer (Nano eNabler, BioForce Nanosciences) was used to print antibodies into the microwells [7]. Before printing, the exposed PC surface was coated using the aldehyde functional group to immobilize antibodies. The printings of antibodies were carried out inside an environmental chamber with the constant humidity of 60%. Fig. 3(c) lists the materials printed at different rows (from row 1 to 12) of the microarray. The microwells of each row were printed with the same material. The antibodies were mixed with the protein printing buffer (BioForce Nanosciences) in a ratio of 50:50% (v/v). In each microwell, the sample volume was approximately 6 pL. Between the nearby rows of antibodies, there was one blank row, which functioned as the reference spots.

C. Hyperspectral imaging setup

To measure the resonance wavelength, λ , of each microwell, a hyperspectral imaging scheme was adopted. Fig. 4(a) shows the hyperspectral imaging setup schematically. A monochromator was used to scan the wavelength of the collimated excitation. The monochromatic excitation was polarized and shrined through the PC-based EV microarray. The transmission image was captured using a microscope (IX-81, Olympus) with a 4× objective and a CCD camera (C9100, Hamamatsu). The monochromator was tuned from 840 nm to 850 nm with the increment of 0.5 nm. The bandwidth of the

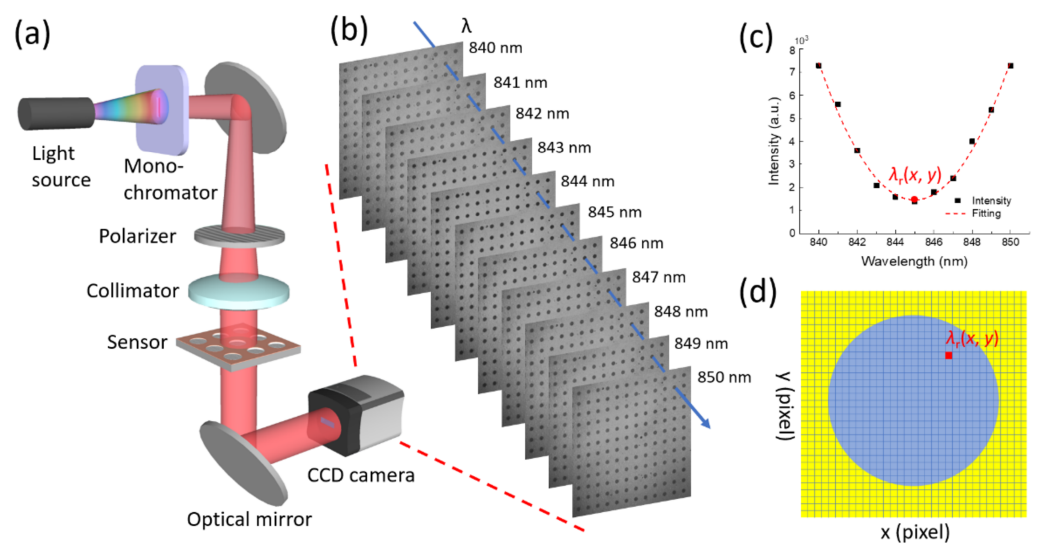


Fig. 4 Label-free imaging scheme for the EV microarray. (a) Schematic diagram of the hyperspectral imaging-based detection setup. (b) Intensity images captured at 11 different wavelengths ranging from 840 nm to 850 nm. Each image consists of 1000×1000 pixels with the spatial pixel resolution of 1.8 μ m. (c) Reconstructed transmission spectrum at a given pixel in the area of interest. The resonance wavelength of this pixel, $\lambda_r(x, y)$, is determined by a curve fitting algorithm. (d) Schematic plot of the label-free image around a single microwell.

monochromatic light was controlled using the slit size. For each wavelength, the transmission image of the EV microarray was recorded by the CCD. Fig. 4(b) shows the serial of monochromatic images captured at the 11 wavelengths. The wavelength range of 840 nm to 850 nm was selected to cover the resonance wavelength during the assay. Fig. 4(c) plots the transmission intensity as a function of wavelength for a given pixel at (x, y) of the EV microarray. The resonance wavelength $\lambda(x, y)$ was determined by fitting the transmission curve, as shown by the red dashed line in fig. 4(c). There were 1000×1000 pixels in each EV microarray image, and the resonance wavelength for all these pixels was calculated to build the label-free image. Fig. 4(d) illustrates the pixelized label-free image consisting of $\lambda(x, y)$ values around a single microwell. The blue spot and yellow area represent the regions inside the microwell and photoresist layer, respectively.

III. RESULTS AND DISCUSSION

Major steps of the label-free EV detection assay are summarized in fig. 5(a). To capture the target EVs, the PC sensor surface was functionalized using a four-step protocol. The blank PC microarray was cleaned and subsequentially coated with polyvinylamine and glutaraldehyde (step 1). The capture antibodies were printed at the concentration of at 0.5 mg mL⁴ (step 2) and were incubated for 4 hours. After the incubation, the microarray was washed in a phosphate buffered saline (PBS) solution to remove the excessive antibodies. Next, the microarray was blocked using bovine serum albumin (BSA, 1 mg mL⁴) to prevent non-specific bindings (step 3). The BSA blocked microarray was used to measure EV bindings to the antibodies.

During the EV detection experiment, label-free images of the array were measured after each step shown in fig. 5(a). Fig. 5(b) shows the label-free microarray image measured after the

printing of antibodies and before the BSA blocking step. The pseudo-color plot represents the resonance wavelength for the pixels inside the microwells. Since the region out of the microwave was covered by the photoresist, the resonance wavelength of the region was manually set at 1000 nm. The box plot in fig. 5(c) shows the resonance wavelength shifts for the panel of antibodies, including CD9, CD63, CD68, CD80, CD81, CD86, and I-A/I-E. Bars indicate the mean The 25th and 75th percentiles and lines indicate the mean ± 1.5 times the interquartile range. For each antibody, the $\Delta\lambda$ values were calculated by subtracting of the reference spot from the nearby sample spot to the and averaging the row of 12 spots.

The macrophage-derived EVs sample was added and incubated on the EV microarray for 3 hours. The concentration and volume of the EV sample were $2\times10^{\circ}$ particles mL $^{\circ}$ and 1 μ L, respectively. Fig. 5(d) is the label-free image after the EVs absorption. Fig. 5(e) compares the resonance wavelength shifts of EV bindings with regard to each antibody. The label-free image measured after the BSA blocking step was used as the baseline to calculate the resonance wavelength shifts. The $\Delta\lambda$ for anti-CD9 is highest, and anti-I-A/I-E is lowest.

We are studying the change of EV membrane protein constituents when the macrophages are active using cytokines and bacterial endotoxins. The results will be reported at the conference.

ACKNOWLEDGMENT

This work was supported by the National Science Foundation under Grant Nos. ECCS 17-11839 and ECCS 16-53673. Any opinions, findings, and conclusions or recommendations expressed in this material are those of the authors and do not necessarily reflect the views of the National Science Foundation.

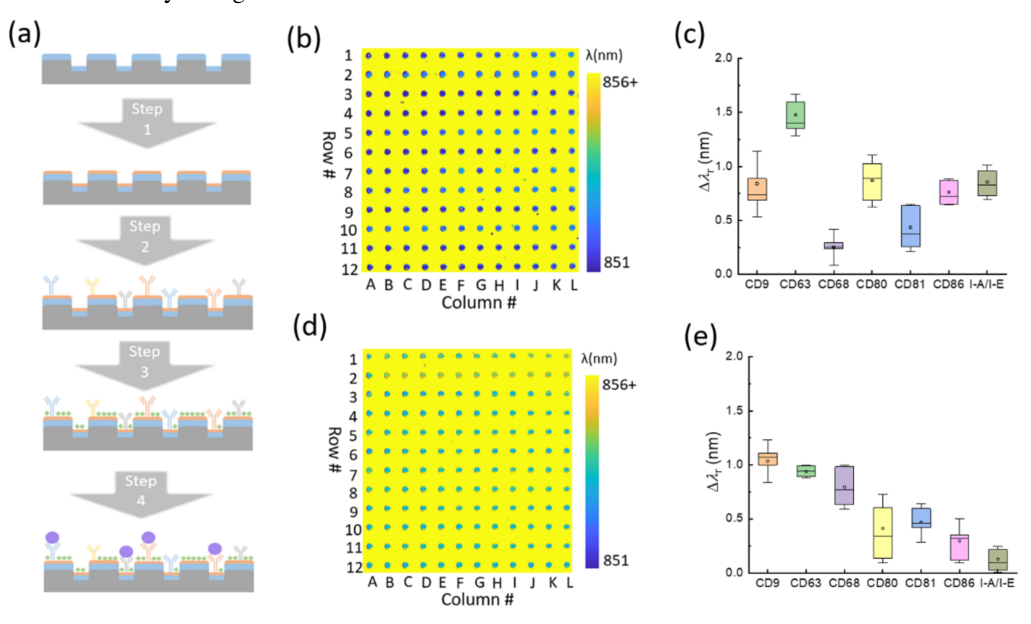


Fig. 5 Label-free microarray for multiplexed analysis of EVs. (a) Schematic flowchart for the label-free EV assay using a PC biosensor. The surface functionalization and blocking processes are shown in Step 1-3. (b) Label-free image of the EV microarray after the printing of antibodies. (c) Box plot of the resonance wavelength shifts for each antibody. (d) Label-free image of the EV bindings. (e) Box plot of the resonance shifts caused by the binding of EVs to each antibody on the EV microarray.

REFERENCES

- H. Im, H. L. Shao, Y. I. Park, V. M. Peterson, C. M. Castro, R. Weissleder, et al., "Label-free detection and molecular profiling of exosomes with a nano-plasmonic sensor," *Nature Biotechnology*, vol. 32, pp. 490-U219, May 2014.
- [2] S. D. Ibsen, J. Wright, J. M. Lewis, S. Kim, S. Y. Ko, J. Ong, et al., "Rapid Isolation and Detection of Exosomes and Associated Biomarkers from Plasma," ACS Nano, vol. 11, pp. 6641-6651, Jul 2017.
- [3] Y. Wang, W. Yuan, M. Kimber, M. Lu, and L. Dong, "Rapid Differentiation of Host and Parasitic Exosome Vesicles Using Microfluidic Photonic Crystal Biosensor," ACS Sensors, vol. 3, pp. 1616-1621. Sep 2018.
- [4] N. De Silva, M. Samblas, J. A. Martinez, and F. I. Milagro, "Effects of exosomes from LPS-activated macrophages on adipocyte gene expression, differentiation, and insulin-dependent glucose uptake," *Journal of Physiology and Biochemistry*, vol. 74, pp. 559-568, Nov 2018.
- [5] M. Shokooh-Saremi and R. Magnusson, "Properties of two-dimensional resonant reflectors with zero-contrast gratings," *Optics Letters*, vol. 39, pp. 6958-6961, Dec 15 2014.
- [6] Y. Zhuo and B. T. Cunningham, "Label-Free Biosensor Imaging on Photonic Crystal Surfaces," Sensors, vol. 15, pp. 21613-21635, Sep 2015.
- [7] F. Yesilkoy, E. R. Arvelo, Y. Jahani, M. K. Liu, A. Tittl, V. Cevher, et al., "Ultrasensitive hyperspectral imaging and biodetection enabled by dielectric metasurfaces," *Nature Photonics*, vol. 13, pp. 390, Jun 2019.
- [8] W. L. Chen, K. D. Long, M. Lu, V. Chaudhery, H. Yu, J. S. Choi, et al., "Photonic crystal enhanced microscopy for imaging of live cell adhesion," Analyst, vol. 138, pp. 5886-5894, 2013.
- [9] Y. Zhuo, H. Hu, W. Chen, M. Lu, L. Tian, H. Yu, et al., "Single nanoparticle detection using photonic crystal enhanced microscopy," *Analyst*, vol. 139, pp. 1007-1015, 2014.
- [10] V. Chaudhery, S. George, M. Lu, A. Pokhriyal, and B. T. Cunningham, "Nanostructured Surfaces and Detection Instrumentation for Photonic Crystal Enhanced Fluorescence," *Sensors*, vol. 13, pp. 5561-5584, May 2013.
- [11] S. Fan and J. D. Joannopoulos, "Analysis of guided resonances in photonic crystal slabs," *Physical Review B*, vol. 65, Jun 15 2002.
- [12] Y. Wang, Y. Huang, J. X. Sun, S. Pandey, and M. Lu, "Guided-mode-resonance-enhanced measurement of thin-film absorption," *Optics Express*, vol. 23, pp. 28567-28573, Nov 2 2015.
- [13] Y. Wang, M. A. Ali, E. K. C. Chow, L. Dong, and M. Lu, "An optofluidic metasurface for lateral flow-through detection of breast cancer biomarker," *Biosensors & Bioelectronics*, vol. 107, pp. 224-229, Jun 1 2018.